

Pomosynthesis and biological activity of silver nanoparticles using *Passiflora tripartita* fruit extracts

Brajesh Kumar^{1*}, Kumari Smita¹, Luis Cumbal^{1*}, Alexis Debut¹, Javier Camacho^{1,2}, Elisabeth Hernández-Gallegos², María de Guadalupe Chávez-López², Marcelo Grijalva¹, Yolanda Angulo¹, Gustavo Rosero¹

¹Centro de Nanociencia y Nanotecnología, Universidad de las Fuerzas Armadas -ESPE, Av. Gral. Rumiñahui s/n, Sangolquí, P.O. BOX 171-5-231B, Ecuador

²Centro de Investigación y de Estudios Avanzados del Instituto Politécnico Nacional, Departamento de Farmacología. C.P. 07360, Mexico City, Mexico

*Corresponding author. Tel: (+593) 2 3989492; E-mail: krmbraj@gmail.com, lhcumbal@espe.edu.ec

Received: 09 August 2014, Revised: 05 November 2014 and Accepted: 15 November 2014

ABSTRACT

Silver nanoparticles (AgNPs) have been synthesized via the green pomosynthetic procedure, using *Passiflora tripartita* var. mollissima fruit pigments as both the reducing and stabilizing agents. UV-Vis Spectroscopy, Dynamic Light Scattering, Transmission Electron Microscopy with Selected Area Electron Diffraction and Powder X-Ray Diffraction are used to completely characterize the AgNPs. The prepared AgNPs are found to be mostly spherical shapes with an average diameter of 49.7 ± 24.6 nm at room temperature. XRD analysis revealed the face-centered cubic geometry of AgNPs whereas Infrared spectrum and cyclic voltammetry measurements hypothesize the possible biomolecules (flavonoid C & O-glycosides) responsible for stabilization of the AgNPs. Synthesized AgNPs shows significant antioxidant efficacy (67%, 0.15 mM) against 1, 1-diphenyl-2-picrylhydrazyl. The AgNPs (0.01 – 20 μ M) did not affect cell proliferation of the human cancer cell lines A-549 and HeLa, from lung and cervix, respectively. The use of environmentally benign, cost-effective and renewable materials like *P. tripartita* extract offers numerous benefits of eco-friendliness and compatibility for potential future pharmaceutical and biomedical applications. Copyright © 2015 VBRI press.

Keywords: Silver nanoparticles; *Passiflora tripartita*; TEM; XRD; antioxidant; cancer cells.



Brajesh Kumar is currently working as a Prometeo Researcher in the Centro de Nanociencia y Nanotecnología, Universidad de las Fuerzas Armadas -ESPE, Ecuador. He received his M.Sc and Ph.D in Chemistry from the University of Delhi, Delhi, India. His research interest is the development of sustainable and ecofriendly technique for natural product extraction, purification and analysis, plant mediated synthesis of nanoparticle and their applications, natural polymers, peptide chemistry, microwave and ultrasound assisted organic

synthesis. He worked as a faculty member in different universities in India, South Korea and published several international research articles, patents and conference paper.



Luis Cumbal-Flores earned BS in Mechanical Engineering from the Polytechnic School of Army (ESPE) -Ecuador. For graduate studies, he attended to Lehigh University, PA, USA and was awarded with MS and PhD in Environmental Engineering. Currently, he is the Director of the Nanoscience and Nanotechnology Center and a professor of the Dept of Life Sciences at ESPE. He and his students synthesize and apply novel nanomaterials for environmental remediation,

active films of organic solar cells, and highly resistant nanostructured polymers for body protection elements. He is the author of a couple of books and several peer-reviewed papers.

Introduction

Over the past few decades, there has been an increased emphasis on the topic of green synthesis of silver nanoparticles (AgNPs). They can be synthesized by several physical, chemical and biological methods [1–3]. The development of techniques for the controlled synthesis of nanoparticles of well-defined size, shape and surface morphology possess unique electrical, optical as well as biological properties. These are applied in catalysis, biosensing, imaging, drug delivery, nanodevice fabrication and in medicine [1, 4, 5]. Environmentally benign and cost-effective procedures for the synthesis of nanoparticles are of interest to the chemist, biologist and material scientist. The work reported all over the world on the role of plant extracts, enzymes, bacteria, biodegradable polymers and

microwaves in the synthesis of nanoparticles has been reviewed by Deepika et al. [6]. Green synthesis of AgNps using *Plukenetia volubilis* shell biomass [7], oil [8] and leaf extract [9], *Capsicum annum* L. extract [10], seed extract of *Jatropha curcas* [11], *Cinnamom zeylanicum* bark extract [12], starch [13], *Hibiscus Rosa sinensis* [14], leaf extract of *Ocimum sanctum* [15], peel extract of *Citrus sinensis* [16], Aloe vera [17], *Nelumbo nucifera* leaf extract [18] and papaya fruit extract [19] have been reported.

The banana passion fruit, known in Ecuador as “taxo & tumbo” (*Passiflora tripartita* var. *mollissima*) belongs to the Passifloraceae plant family comprises around 530 species originated from temperate and tropical South America [20]. The aromatic fruits consumed from prehispanic times, are very appreciated for the pleasant taste and acidic fruit juice. On the basis of the available literature, we hypothesized that pulp of a fruit contains luteolin and apigenin derivatives as isoorientin, orientin and isovitexin [21-23] could be used for the synthesis of silver nanoparticles. However, there is no report on the pomsynthesis of AgNPs using *P. tripartita* fruit and their biological applications.

In the present work, first time AgNps were synthesized by using the extract of *P. tripartita* fruit and the prepared AgNPs were characterized by various analytical techniques. The green synthesized AgNPs exhibited effective (a) *in vitro* free radical scavenging efficacy against 1, 1-diphenyl-2-picrylhydrazyl and (b) cell proliferation of the human cancer cell lines A-549 and HeLa, from lung and cervix, respectively.

Experimental

Materials

The yellow *P. tripartita* (TAXO) used in this experiment was fresh, ripened, and was purchased from the local market Sangolqui, near Universidad de las Fuerzas Armadas -ESPE, Ecuador. Silver nitrate (AgNO_3 , 99.5%) was purchased from Spectrum, USA and 1, 1-diphenyl-2-picrylhydrazyl (DPPH, 99.5%) was purchased from Aldrich, USA. The human cancer cell lines A-549 and HeLa from lung and cervix, respectively, were obtained from the American Type Culture Collection (ATCC; Manassas, VA, USA) and cultured following the manufacturer's instructions. The 3-(4, 5-dimethylthiazol-2-yl)-2, 5-diphenyltetrazolium bromide (MTT) cell proliferation kit I was purchased from Boehringer Mannheim GmbH, Germany.

Preparation of *Passiflora tripartita* fruit extract

A 25 g of thoroughly washed *P. tripartita* fruit (whole part) was chopped finely, and sonication in 70 mL mixture of methanol and double distilled water (1/1) for 10 min. The yellow extract was filtered through a Whatmann filter paper No. 2. The clear filtrate was used for the synthesis of silver nanoparticles and stored at 4 °C for further experiments.

Synthesis of silver nanoparticles

For all experiments, the source of the silver was silver nitrate (AgNO_3 , 1 mM) within double distilled water. Typical reaction mixtures contained 0.1 mL of *P. tripartita*

extract in 10 mL of AgNO_3 solution (1mM) at room temperature. The reaction mixtures were monitored at different time intervals and the nanoparticles that were formed were characterized further. The effect of the silver salt was determined by varying the concentration of silver nitrate (0.1 mM, 1mM and 10 mM). The *P. tripartita* extract was varied (0.1, 0.2, 0.3, 0.5 or 1.0 ml) while keeping the standard silver nitrate concentration at a level of 1 mM.

Characterization of silver nanoparticles

The synthesized AgNps were characterized with the help of a UV-Vis spectrophotometer (Thermospectronic, GENESYS™ 8). Size of nanoparticles was analyzed by using Dynamic Light Scattering instrument (HORIBA LB - 550). Transmission Electron Microscopy was performed on support film of 2% polyvinyl formal solution stabilized with carbon. Briefly, TEM and SAED Images were recorded digitally (FEI Tecnai G2 spirit twin). X-ray diffraction (XRD) studies on thin films of the nanoparticle were carried out using a BRUKER D8 ADVANCE brand θ - 2θ configuration (generator-detector) x-ray tube copper $\lambda = 1.54 \text{ \AA}$ and LYNXEYE PSD detector. FTIR analysis was carried out to determine the functional groups present in *P. tripartita* extract and their possible involvement in the synthesis of AgNps. The FTIR-ATR spectra were collected in the transmission mode ($4000\text{--}650 \text{ cm}^{-1}$) using a Perkin Elmer spectrophotometer (FTIR Spectrum Two). Electrochemical measurements were carried out with a compact potentiostat DY2100 coupled to a personal computer with the DY21008 software installed. Cyclic Voltammetry (CV) measurements were done using a three-electrode system. The working electrode is a glassy carbon electrode with a calomet (Hg/HgCl) electrode as reference. A platinum strand served as the auxiliary electrode. The glassy carbon working electrode was polished with $0.05 \mu\text{m}$ alumina powder before each scanning. The analyses were realized in 0.1M KCl solution. Prior to each run, the dissolved oxygen in KCl solutions was removed by bubbling with N_2 for about 15 min. Voltammetry scan rate were of 5mVs^{-1} at room temperature in the range from -1.2 to 1.2V vs. (SHE vs. SCE). The data were analyzed by using the program Origin v.8.

Antioxidant activity

The *in vitro* scavenging activity of the AgNPs was measured by using DPPH as a free radical model and a method adapted from Magalhaes et al., 2014 with slight modification [24]. An aliquot (1.0- 0.2 mL) of AgNPs or control and (1.0 -1.8 mL) of H_2O was mixed with 2.0 mL of 0.2 mM (DPPH) in absolute methanol. The mixture was vortexed vigorously and allowed to stand at room temperature for 30 min in the dark. Absorbance of the mixture was measured spectrophotometrically at 517 nm, and the free radical scavenging activity was calculated using Eq. (1):

$$\text{Scavenging effect (\%)} = [1 - \{\text{absorbance of sample} / \text{absorbance of control}\}] \times 100 \quad (1)$$

The scavenging percentage of all samples was plotted. The final result was expressed as % of DPPH free radical scavenging activity (mM).

Cell culture and proliferation assays

Cell proliferation was assessed with the colorimetric method based on the conversion of tetrazolium salts to formazan crystals by dehydrogenase activity in active mitochondria as previously described by Chávez-López et al., 2014 [25]. Briefly, Both 4,000 cells / well were seeded in 96-well plates and cell lines were grown incubated for 48 hours in the absence (control) or presence of AgNPs (0.01 – 20 μ M). MTT (0.5 mg / mL) was added 4 hours before the end of the incubation time. The absorbance was obtained from the resulting colored solution with an ELISA plate reader (Multiskan FC, ThermoScientific v 10094). The average absorbance of each individual culture was obtained by measuring 14 different wells for each concentration. Three different cultures were performed per cell line.

Statistical Analysis: ANOVA followed by Tukey-Kramer test was performed. P values < 0.05 were considered statistically significant. The analysis was performed using GraphPad Prism version 5.0 software.

Results and discussion

UV-visible and visual studies

The UV-Vis spectrum of the *P. tripartita* extract is shown in the inset **Fig. 1 (a)**; the peaks are typical of the absorptions of phenolic content, flavonoid C-glycosides and O-glycoside derivatives. The peak at 260 nm was assigned to the strong absorption of phenolic content in the extract [23]. The absorption at 440 nm flavonoid C-glycosides and O-glycoside derivatives are known to interact with silver ions. Fig. 1a displays the UV-Vis spectra of solution (1) as a function of reaction time. The strong resonance centered at 440 nm was clearly observed and increased in intensity with time. It might arise from the excitation of longitudinal plasmon vibrations in AgNPs [13] in the solution.

Fig. 2 (b) presents a plot of the plasmon intensity at 440 nm against reaction time. It can be seen easily that the plasmon intensity at the reaction time of 30 days is near to that at 46 days, meaning completion of the reaction. The insets of **Fig. 1 (b)** present the color changes in the mixture solution over the reaction time. The extract was light pink after reaction with silver ions (1) and changed to light brown (2, 3, 4, 5) and dark brown (6, 7) after reaction times of 2 hrs, 4 hrs, 4 days, 10 days, 17 days, 30 days and 46 days respectively, and then the color did not change any more with reaction time. The characteristic brown color of silver solutions provided a convenient spectroscopic signature to indicate their formation.

TEM and DLS studies

The TEM images of AgNPs and the SAED pattern recorded after 30 days of reaction time are depicted in **Fig. 2 (a-c)**. From the images, it can be seen that the average size of the AgNPs was around 20–50 nm with spherical, triangular and decahedral shapes. The SAED pattern reveals that the

synthesized AgNPs are crystalline. In order to determine the particle size distribution of AgNPs in solution, DLS measurements were carried out after 30 days of reaction time. The qualitative DLS size distribution image of AgNPs is shown in **Fig. 2 (d)**. The average particle sizes of AgNPs size = 49.7 nm and σ = 24.6 nm, respectively. From the results of the DLS study, it could be inferred that the size of AgNPs coincides with the TEM results.

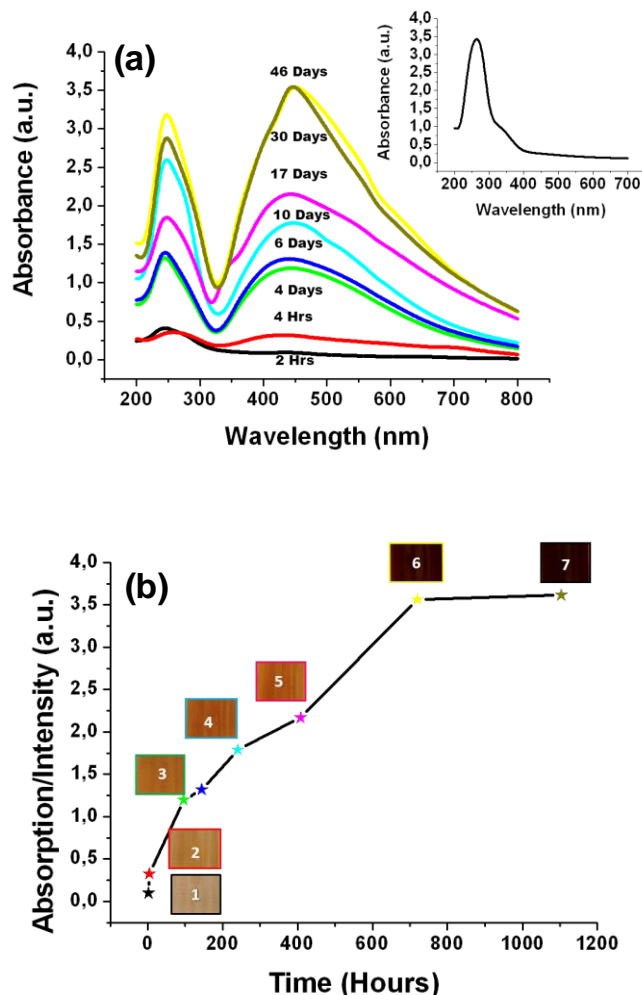


Fig. 1. (a) The UV-Vis absorbance spectrum of AgNPs ($\lambda_{max} = 440$ nm); the inset is the UV-vis spectrum of *P. tripartita* extract and (b) Plot of the intensity of the UV-Vis absorbance at 440 nm against the reaction time; the insets are photos of the solution changes with reaction time (1, 2, 3, 4, 5, 6 and 7 at 2 hrs, 4 hrs, 4 days, 10 days, 17 days, 30 days and 46 days).

XRD studies

The X-ray diffraction patterns of the synthesized AgNPs are shown in **Fig. 3**. The indexing process of a powder diffraction pattern is done and Miller Indices (h, k l) to each peak is assigned in the first step. A number of strong Bragg reflections can be seen which correspond to the (111), (200), (220) and (311) reflections of fcc silver. All the reflections correspond to pure silver metal with face centered cubic symmetry. The high intense peak for FCC materials is generally (111) reflection, which is observed in the sample. The ratio between the intensity of the (200) and (111) diffraction peaks of 0.15 is lower than the conventional bulk intensity ratio 0.40, suggesting that the (111) plane is the predominant orientation and high degree

of crystallinity. However, the diffraction peaks are broad which indicate that the crystallite size is very small [26]. The XRD shows that AgNPs formed are crystalline. Four peaks at 2θ values of 38.138, 44.264, 64.440 and 77.363 deg corresponding to (111), (200), (220) and (311) planes of silver is observed and compared with the standard powder diffraction card of the Joint Committee on Powder Diffraction Standards (JCPDS), silver file No. 04-0783. The XRD study confirms that the resultant particles are (fcc) AgNps.

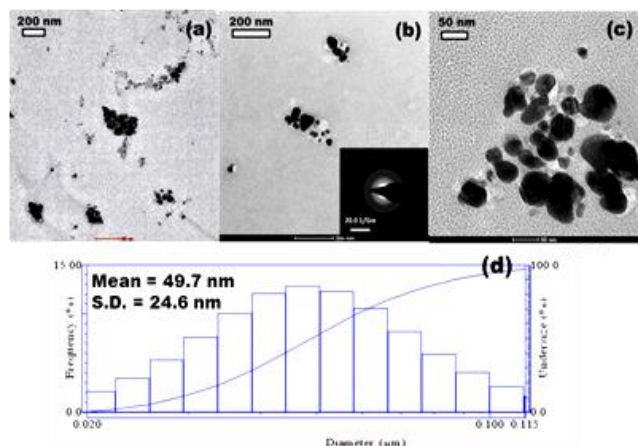


Fig. 2. Typical (a-c) TEM image with SAED pattern and (d) histogram showing the size distribution of AgNps.

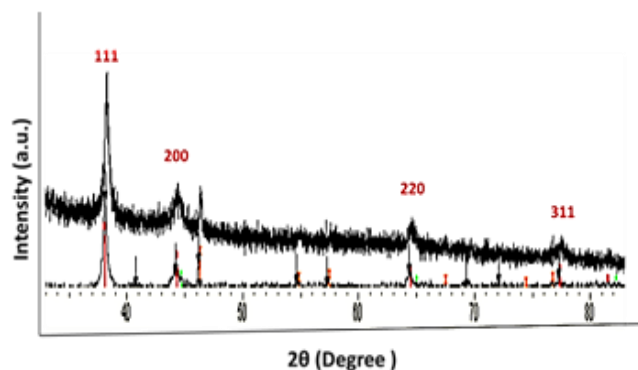


Fig. 3. XRD patterns of AgNps synthesized by using *P. tripartita* extract.

FTIR and Cyclic voltametry Studies

In order to predict the functional groups on *P. tripartita* pigment and their role in the synthesis of AgNps, FTIR and Cyclic voltametry analysis were performed. The control FTIR spectra (untreated with silver nitrate) showed a number of peaks thus reflecting a complex nature of the *P. tripartita* pigment. The band intensities in different regions of the spectrum, before and after reaction with silver nitrate were analyzed and are shown in Fig. 4 (a, b). There was a deviation in the following peaks: 3339–3326, 1654–1637, 1449–1443, 1410–1412 and 1019–1020 cm^{-1} . The peak located at around 3339 cm^{-1} was attributed to the O-H, either alcoholic or polyphenolic stretching and those at 2946–2834 cm^{-1} indicated C-H (aliphatic) stretching. The peak shift from 3339 to 3326 cm^{-1} implies that these groups may be involved in the process of nanoparticle synthesis via intermolecular H-bonding. The peak located at 1654 cm^{-1} could be assigned to the C=O stretching in carboxyl or

C=C-C=O stretching in the conjugated carboxyl. A shift in this peak (from 1654 to 1637 cm^{-1}) indicates the possible involvement of carboxyl or conjugated carboxyl in nanoparticle synthesis (due to disruption of conjugated system). The vibration shift around 1449–1443 cm^{-1} was suggestive of the involvement of aliphatic and aromatic (C-H) plane deformation vibrations of methyl, methylene and methoxy groups in the reductive process. Peak observed at 1019 cm^{-1} corresponds to secondary -OH stretching, indicating that the secondary -OH also participates in nanoparticles synthesis. *P. tripartita* pigments are mainly composed of glucose, C-glycosides and O-glycoside derivatives as functional groups [23], may be involved in reducing the Ag^+ to Ag^0 .

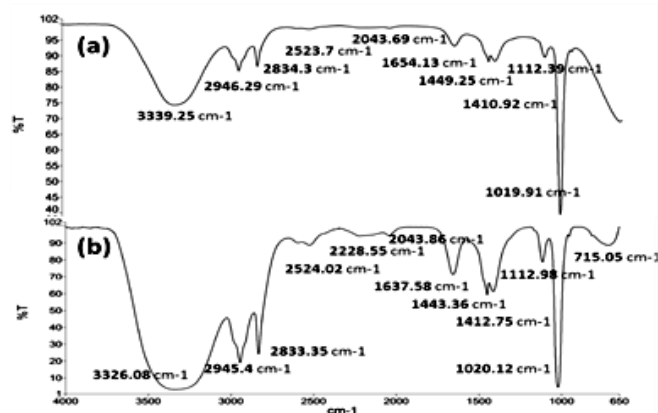


Fig. 4. FTIR spectra of (a) *P. tripartita* extract and (b) AgNps.

Fig. 5 (a, b) shows differential voltammograms obtained of the taxo pigment before and after the process of the biosynthesis of the AgNps, inset shows the background of the CV signal of the anodic waves from taxo pigment with or without nanoparticles. It is possible to observe that CVs peaks correspond to a sequent oxidation of the hydroxyl groups of the anodic wave. These peaks could be the presence of a mixture of flavonoids in the structural chemistry of the taxo pigment [27].

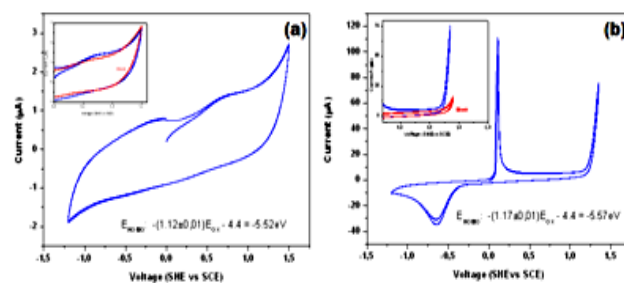


Fig. 5. Cyclic voltammetry of (a) *P. tripartita* extract and (b) AgNps with glassy carbon working electrode, calomet (Hg/HgCl) electrode as reference and platinum strand served as the auxiliary electrode. Potential range from -1.2 to 1.2V vs (SHE vs.SCE), Scan rate: 5mVs⁻¹.

According to the literature, the possible flavonoids, apigenin or naringenin were the responsible of passage of current in the taxo pigment [27]. Parameters indicate the anodic current of the samples and its similitude of these flavonoids, were determined as indicated in the literature [27], such as the peak potentials (E_p) is 0.69V, the peak current densities (i_p) are 6.92 $\mu\text{A}/\text{cm}^2$ and the charge below

voltammetric waves (Q_p) is $0.53\mu\text{C}/\text{cm}^2$ as shown in **Fig. 5 (a)**. On the other hand, in the CV of **Fig. 5 (b)**, shows peaks characteristics of AgNPs of silver in the cathode wave. In these CVs is possible to show a decrease the peak in the anodic wave or disappear after the process of the biosynthesis of the AgNPs.

From FTIR and CV results, we concluded that the biological components are known to interact with metal salts (Ag^+) via these functional groups and mediate their reduction to nanoparticles (Ag^0) as shown in **Fig. 6**.

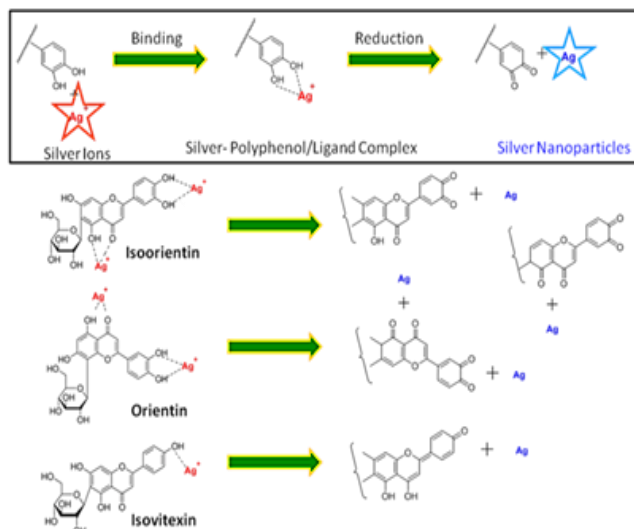


Fig. 6. The proposed mechanism for synthesis of AgNPs using biomolecules of *P. tripartita*.

Antioxidant activities

In the present study, DPPH was first used as a preliminary radical scavenging activity test. In the DPPH method, the antioxidant reacts with the stable DPPH (deep violet color) and converts it into 1, 1-diphenyl-2-picrylhydrazine with discoloration (light yellow color). The percentage of free radical scavenging activity at different concentration ranging from 0.05 to 0.25 mM for the AgNPs was evaluated. It was found that, the efficacy of AgNPs higher at concentration 0.15 mM at the same *in vitro* condition (**Fig. 7**). The antioxidant activity increases with increasing volume and maximum at 65.9 % for 0.10 mM and 66.93 % for 0.15 mM AgNPs. The antioxidant efficacy against DPPH is probably derived, through the electrostatic attraction between negatively charged bioactive compounds (COO^- , O^-) and neutral or positively charged nanoparticles. AgNPs bound to the phytochemicals and their bioactivity increases by synergistically. The effect of activity depends on the site of attachment of the metals and its consequent impact on the activity of the antioxidant agent [28].

Cancer cell proliferation

In vitro cytotoxicity of the AgNPs was evaluated against human cancer cell lines A-549 and HeLa, from lung and cervix at different concentrations (0.01 – 20 μM). **Fig. 8** shows no effect of AgNPs on cell proliferation of lung A-549 or HeLa cervical cells. Despite the cell internalization of AgNPs should be studied, and additional biological test

could be performed, these results suggest that the new AgNPs might be used as safe carriers.

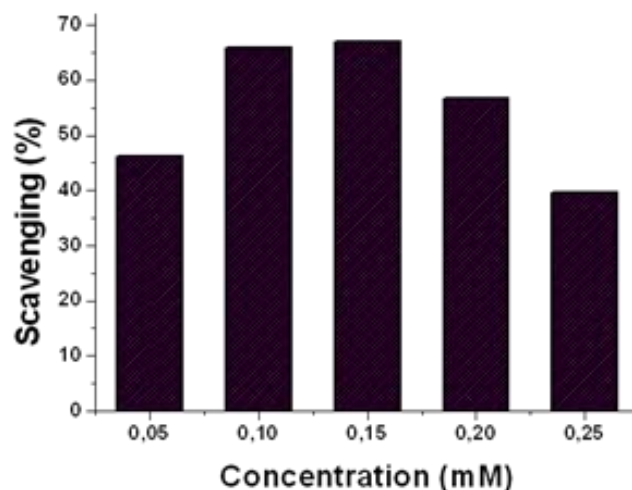


Fig. 7. The Antioxidant efficacy of AgNPs against DPPH.

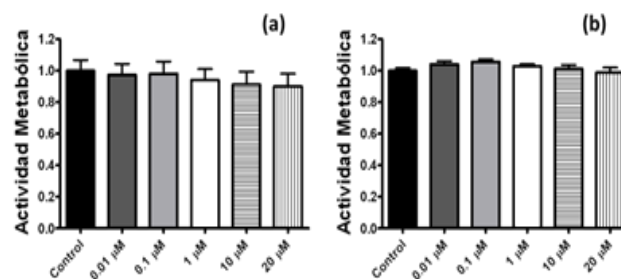


Fig. 8. Effect of AgNPs on cell proliferation. AgNPs did not affect cell proliferation of (a) A-549 lung cancer, or (b) HeLa cervical carcinoma cells. Mean \pm S.D. of 3 different cultures are shown.

Conclusion

In conclusion, we describe a simple procedure for the pomsynthesis of AgNPs with several advantages such as cost-effectiveness, compatibility for biomedical and pharmaceutical applications as well as for large-scale commercial production. The phytoconstituents such as flavonoid *C*-glycosides and *O*-glycoside derivatives act as reducing and capping agents for the synthesis of AgNPs, are evident from FT-IR and CV studies. TEM analysis showed that the synthesized stable AgNPs are approximately 24–50 nm in size with spherical, triangle and decahedral shapes. XRD and SAED analysis revealed the face-centered cubic geometry and crystalline nature of the AgNPs. To this end, *in vitro* radical scavenging activity of synthesized AgNPs against DPPH was remarkable (67%, 0.15 mM) and AgNPs did not affect the proliferation of cancer cells in the concentration range tested (0.01 – 20 μM). This study encourages the use of *P. tripartita* and other Andean edible fruits as new crops for synthesis of nanoparticles with potential future pharmaceutical and biomedical applications in worldwide.

Acknowledgements

This scientific work has been funded by the Prometeo Project of the National Secretariat of Higher Education, Science, Technology and Innovation (SENESCYT), Ecuador.

Reference

- Nair, L.S.; Laurencin, C.T. *J. Biomed. Nanotechnol.*, **2007**, *3*, 301.
DOI: [10.1166/jbn.2007.041](https://doi.org/10.1166/jbn.2007.041)
- Zhang, Y.; Peng, H.; Huang, W.; Zhou, Y.; Yan, D. *Colloids Interface Sci.*, **2008**, *325*, 371.
DOI: [10.1016/j.cis.2008.05.063](https://doi.org/10.1016/j.cis.2008.05.063)
- Sharma, V.K.; Yngard, R.A.; Lin, Y. *Adv. Colloid Interface Sci.*, **2009**, *145*, 83.
DOI: [10.1016/j.cis.2008.09.002](https://doi.org/10.1016/j.cis.2008.09.002)
- Lee, K.S.; El-Sayed, M.A. *J Phys. Chem. B*, **2006**, *110*, 19220.
DOI: [10.1021/jp062536y](https://doi.org/10.1021/jp062536y)
- Jain, P.K.; Huang, X.; El-Sayed, I.H.; EL-Sayed, M.A. *Acc. Chem. Res.*, **2008**, *41*, 1578.
DOI: [10.1021/ar7002804](https://doi.org/10.1021/ar7002804)
- Hebbalalu, D.; Lalley, J.; Nadagouda, M.N.; Varma, R.S. *ACS Sustainable Chem. Eng.*, **2013**, *1*, 703.
DOI: [10.1021/sc4000362](https://doi.org/10.1021/sc4000362)
- Kumar, B.; Smita, K.; Cumbal, L.; Debut, A. *J. Saudi Chem. Soc.*, 2014, article in press,
DOI: [10.1016/j.jscs.2014.03.005](https://doi.org/10.1016/j.jscs.2014.03.005)
- Kumar, B.; Smita, K.; Cumbal, L.; Debut, A. *Ind Crops Prod*, **2014**, *58*, 238.
DOI: [10.1016/j.indcrop.2014.04.021](https://doi.org/10.1016/j.indcrop.2014.04.021)
- Kumar, B.; Smita, K.; Cumbal, L.; Debut, A. *Saudi J Biol Sci*, **2014**, *21*, 605.
DOI: [10.1016/j.sjbs.2014.07.004](https://doi.org/10.1016/j.sjbs.2014.07.004)
- Li, S.; Shen, Y.; Xie, A.; Yu, X.; Qiu, L.; Zhang, L.; Zhang, Q. *Green Chem*, **2007**, *9*, 852.
DOI: [10.1039/B615357G](https://doi.org/10.1039/B615357G)
- Bar, H.; Bhui, D.K.; Sahoo, G.P.; Sarkar, P.; Pyne, S.; Misra, A. *Colloids and Surfaces A: Physicochem. Eng. Aspects*, **2009**, *348*, 212.
DOI: [10.1016/j.colsurfa.2009.07.021](https://doi.org/10.1016/j.colsurfa.2009.07.021)
- Sathishkumar, M.; Sneha, K.; Won, S.W.; Cho, C.-W.; Kim, S.; Yun, Y.-S. *Colloids and Surfaces B: Biointerfaces*, **2009**, *73*, 332.
DOI: [10.1016/j.colsurfb.2009.06.005](https://doi.org/10.1016/j.colsurfb.2009.06.005)
- Kumar, B.; Smita, K.; Cumbal, L.; Debut, A.; Pathak, R.N. *Bioinorg Chem Appl* (2014) Article ID 784268.
DOI: [10.1155/2014/784268](https://doi.org/10.1155/2014/784268)
- Philip, D. *Physica E*, **2010**, *42*, 1417.
DOI: [10.1016/j.physe.2009.11.081](https://doi.org/10.1016/j.physe.2009.11.081)
- Singhal, G.; Bhavesh, R.; Kasariya, K.; Sharma, A.R.; Singh, R.P. *J Nanopart Res*, **2011**, *13*, 2981.
DOI: [10.1007/s11051-010-0193-y](https://doi.org/10.1007/s11051-010-0193-y)
- Kaviya, S.; Santhanalakshmi, J.; Viswanathan, B.; Muthumary, J.; Srinivasan, K. *Spectrochim. Acta, Part A*, **2011**, *79*, 594.
DOI: [10.1016/j.saa.2011.03.040](https://doi.org/10.1016/j.saa.2011.03.040)
- Chandran, S.P.; Chaudhary, M.; Pasricha, R.; Ahmad, A.; Sastry, M. *Biotechnol. Prog.*, **2006**, *22*, 577.
DOI: [10.1021/bp0501423](https://doi.org/10.1021/bp0501423)
- Santhoshkumar, T.; Rahuman, A.A.; Rajakumar, G.; Marimuthu, S.; Bagavan, A.; Jayaseelan, C.; Zahir, A.A.; Elango, G.; Kamaraj, C. *Parasitol. Res.*, **2011**, *108*, 693.
DOI: [10.1007/s00436-010-2115-4](https://doi.org/10.1007/s00436-010-2115-4)
- Jain, D.; Daima, H.K.; Kachhwaha, S.; Kothari, S.L. *Dig. J. Nanomater. Biostruct.*, **2009**, *4*, 557.
- Chassagne, D.; Boulanger, R.; Crouzet, J. *Food Chemistry*, **1999**, *66*, 281.
DOI: [10.1016/S0308-8146\(99\)00044-8](https://doi.org/10.1016/S0308-8146(99)00044-8)
- Zucolotto, S.M.; Fagundes, C.; Reginatto, F.H.; Ramos, F.A.; Castellanos, L.; Duque, C.; Schenkel, E.P. *Phytochem. Anal.*, **2012**, *23*, 232.
DOI: [10.1002/pca.1348](https://doi.org/10.1002/pca.1348)
- Ramos, F.A.R.; Castellanos, L.; Lopez, C.; Palacios, L.; Duque, C.; Pacheco, R.; Guzman, A. *Lat. Am. J. Pharm.*, **2010**, *29*, 141.
DOI: <http://sedici.unlp.edu.ar/handle/10915/7884>
- Simirgiotis, M.J.; Hirschmann, G.S.; Bórquez, J.; Kennelly, E.J. *Molecules*, **2013**, *18*, 1672.
DOI: [10.3390/molecules18021672](https://doi.org/10.3390/molecules18021672)
- Magalhaes, L.M.; Segundo, M.A.; Reis, S.; Lima, J.L.F.C. *Analytica Chimica Acta*, **2006**, *558*, 310.
DOI: [10.1016/j.aca.2005.11.013](https://doi.org/10.1016/j.aca.2005.11.013)
- Chávez-López, M.; Hernández-Gallegos, E.; Vázquez-Sánchez, A.Y.; Gariglió, P.; Camacho, J. *Int J Gynecol Cancer.*, **2014**, *24*, 824.
DOI: [10.1097/IGC.0000000000000151](https://doi.org/10.1097/IGC.0000000000000151)
- Wani, I.A.; Ganguly, A.; Ahmed, J.; Ahmad, T. *Mat. Lett.*, **2011**, *65*, 520.
DOI: [10.1016/j.matlet.2010.11.003](https://doi.org/10.1016/j.matlet.2010.11.003)
- Zhang, D.; Chu, L.; Liu, Y.; Wang, A.; Ji, B.; Wu, W.; Zhou, F.; Wei, Y.; Cheng, Q.; Cai, S.; Xie, L.; Jia, G. *J. Agric. Food Chem.*, **2011**, *59*, 10277.
DOI: [10.1021/jf201773q](https://doi.org/10.1021/jf201773q)
- Kumar, B.; Smita, K.; Cumbal, L.; Debut, A. *Bioinorg Chem Appl* (2014) Article ID 523869.
DOI: [10.1155/2014/523869](https://doi.org/10.1155/2014/523869)

Advanced Materials Letters

Publish your article in this journal

ADVANCED MATERIALS Letters is an international journal published quarterly. The journal is intended to provide top-quality peer-reviewed research papers in the fascinating field of materials science particularly in the area of structure, synthesis and processing, characterization, advanced-state properties, and applications of materials. All articles are indexed on various databases including DOI and are available for download for free. The manuscript management system is completely electronic and has fast and fair peer-review process. The journal includes review articles, research articles, notes, letter to editor and short communications.

